Molecular Biology of the Cell
Vol. 16, 5610–5620, December 2005

Nup153 Affects Entry of Messenger and Ribosomal Ribonucleoproteins into the Nuclear Basket during Export[D]

Teresa Soop, Birgitta Ivarsson, Birgitta Björkroth, Nathalie Fomproix, Sergej Masich, Volker C. Cordes,* and Bertil Daneholt

Department of Cell and Molecular Biology, Medical Nobel Institute, Karolinska Institutet, S-171 77 Stockholm, Sweden

Submitted August 3, 2005; Accepted September 15, 2005
Monitoring Editor: Joseph Gall

A specific messenger ribonucleoprotein (RNP) particle, Balbiani ring (BR) granules in the dipteran *Chironomus tentans*, can be visualized during passage through the nuclear pore complex (NPC). We have now examined the transport through the nuclear basket preceding the actual translocation through the NPC. The basket consists of eight fibrils anchored to the NPC core by nucleoprotein Nup153. On nuclear injection of anti-Nup153, the transport of BR granules is blocked. Many granules are retained on top of the nuclear basket, whereas no granules are seen in transit through NPC. Interestingly, the effect of Nup153 seems distant from the antibody-binding site at the base of the basket. We conclude that the entry into the basket is a two-step process: an mRMP first binds to the tip of the basket fibrils and only then is it transferred into the basket by a Nup153-dependent process. It is indicated that ribosomal subunits follow a similar pathway.

INTRODUCTION

RNA molecules are exported from nucleus to cytoplasm as ribonucleoprotein (RNP) complexes (Daneholt, 2001; Dreyfuss *et al*., 2002; Lei and Silver, 2002). The translocation of RNPs through nuclear pores has been visualized in the electron microscope both for messenger RNPs (Stevens and Swift 1966; Mehlin *et al*., 1992; Kiseleva *et al*., 1998) and for ribosomes/ribosomal subunits (Franke and Scheer, 1974). The pores contain a specific supramolecular assembly, the nuclear pore complex (NPC), and the passage occurs through the central channel of the complex (Dworetzky and Feldherr, 1988). During the last decade, it has been revealed that the translocation apparently takes place in discrete steps (Daneholt, 1997). The molecular mechanisms involved are currently being revealed.

The NPC is a three-layered structure with a central spoke assembly sandwiched between a nuclear and cytoplasmic ring (Allen *et al*., 2000; Vasu and Forbes, 2001; Fahrenkrog and Aebi, 2003; Suntharalingam and Wente, 2003). In the center, there is a 25-nm-wide channel filled with a meshwork of very thin fibrils, often designated as the central plug. Additional auxiliary components are attached to the NPC periphery. On the nuclear side, eight longer fibrils emanate from the nuclear ring. At their distal ends, these fibrils seem to bifurcate and laterally interdigitate with their neighboring fibrils, thereby forming another ringlike structure referred to as the terminal ring. Together, nuclear fibrils and terminal ring are considered a structural and functional entity, called the nuclear basket. On the cytoplasmic side, eight short fibrils extend from the cytoplasmic ring into cytoplasm.

The NPC contains ~30 proteins designated nucleoporins, the majority of which are symmetrically organized in the core of the NPC (Rout *et al*., 2000; Cronshaw *et al*., 2002). The central plug material is composed of a group of nucleoporins containing multiple repeats of the dipeptide sequence FG. These repeats are involved in the actual translocation of macromolecules and supramolecular assemblies through the pore (see further below in *Introduction*). Some few nucleoporins are only present on one or the other side of the NPC. The basket fibrils contain a protein called Tpr (Cordes *et al*., 1997; Frosst *et al*., 2002; Krull *et al*., 2004) and are anchored to the nuclear ring by another asymmetrically positioned nucleoporin called Nup153 (Sukegawa and Blobel 1993; Hase and Cordes, 2003).

RNP complexes need specific export receptors that carry them through the nuclear pores (Nakielny and Dreyfuss, 1999; Reed and Hurt, 2002; Stutz and Izaurralde, 2003). The most abundant messenger (m)RNP export receptor consists of the heterodimer NXF1-p15 (in yeast Mex67-Mtr2p). Other RNP complexes, such as ribosomal subunits and small nuclear RNP particles, are carried by members of another major family of transport receptors, the importins/exportins, also known as karyopherins (Cullen, 2003). tRNA, too, is transferred by a specific member of this family, called exportin-t.

This article was published online ahead of print in *MBC in Press* (http://www.molbiolcell.org/cgi/doi/10.1091/mbc.E05–08–0715) on September 29, 2005.

[D] The online version of this article contains supplemental material at *MBC Online* (http://www.molbiolcell.org).

* Present address: Zentrum für Molekulare Biologie, University of Heidelberg, Im Neuenheimer Feld 282, D-69120 Heidelberg, Germany.

Address correspondence to: Bertil Daneholt (bertil.daneholt@cmb.ki.se).

Abbreviations used: BR, Balbiani ring; NE, nuclear envelope; NPC, nuclear pore complex; RNP, ribonucleoprotein; rRNA, ribosomal RNA.

The export receptors bind to their RNA cargo molecule either directly or via an RNA-binding adaptor protein. In mRNA transport, these cargos are linked to their export receptors via members of the REF protein family (yeast homologue Yra1p) (Strässer and Hurt, 2000; Stutz *et al*., 2000) and/or members of the SR protein family (in yeast the SR-like Npl3p) (Huang *et al*., 2003; Gilbert and Guthrie, 2004).

Although structurally different, the various export receptors seem to use the same pathway when translocating through the NPC core. There they interact with the FG-repeat domains of the filamentous nucleoporins in the central NPC channel (Suntharalingam and Wente, 2003). Although FG-repeats are essential for allowing translocation of macromolecular entities through the channel (Strawn *et al*., 2004), the precise translocation mechanism is still unclear (for specific models, see Ribbeck and Görlich 2002; Rout *et al*., 2003). It has been proposed that the directionality of the transport could be accomplished by asymmetrically arranged FG-repeat nucleoporins with different affinities for the transport receptor (Ben-Efraim and Gerace, 2001). However, recent work has shown that FG-repeats of asymmetrically distributed nucleoporins can be deleted or swapped with little effect on the transport (Strawn *et al*., 2004; Zeitler and Weis, 2004). Therefore, presently, it seems more likely that the directionality is accomplished by asymmetric modifications of the export complex at the entrance to the NPC or the exit from this structure (Görlich and Kutay, 1999).

Once the mRNP has been translocated through the NPC proper, its exit and release from the cytoplasmic NPC side might be promoted by the RNA helicase Dbp5. This helicase is likely to restructure the exiting RNP (Snay-Hodge *et al*., 1998, Zhao *et al*., 2002) and therefore could prevent its reentry into the channel. Furthermore, initiation of protein synthesis can be intimately coupled to the exit of mRNA into cytoplasm (Mehlin *et al*., 1992). The extensive exchange of proteins at the 5′ end of the transcript, required for translation, could then also contribute to making the nucleocytoplasmic translocation of an mRNP irreversible.

Less is known about the molecular mechanisms involved in the initial interaction of the RNP complex with the basket and events preceding the translocation through the central channel. It can be seen in the electron microscope how a large mRNP complex moves through the basket, docks in front of the central channel, unfolds, and enters the NPC channel (Mehlin *et al*., 1992; Daneholt, 1997; Kiseleva *et al*., 1998). It has also been revealed that the basket is dynamically rearranged when the particle passes through the terminal ring of the basket (Kiseleva *et al*., 1996), but the significance of these initial steps is unclear.

Tpr, the main constituent of the nuclear basket, is a protein forming coiled-coil homodimers of extended rod-like shape (Hase *et al*., 2001). Studies in mammalian cells point at potential roles in mRNA and nuclear protein export (Bangs *et al*., 1998; Frosst *et al*., 2002). Recently, a Tpr homologue in yeast, Mlp1, has been reported being incapable of selectively retaining nonspliced mRNAs in the nuclear interior (Galy *et al*., 2004).

Nup153, the protein tethering Tpr to the NPC, exhibits a tripartite structure: a zinc-finger domain is flanked by N- and C-terminal domains (Sukegawa and Blobel, 1993). The N-terminal domain includes the Tpr binding site, and the site for its own anchorage to the NPC (Enarson *et al*., 1998; Hase and Cordes 2003). The zinc-finger domain binds RanGDP (Nakielny *et al*., 1999), whereas the C-terminal domain contains numerous FG-repeats. Import and export receptors, such as importin β, transportin 1, and CRM1, interact with several regions of Nup153 in a RanGTP-regulated manner (Shah *et al*., 1998; Nakielny *et al*., 1999).

Several studies have indicated that Nup153 is involved in export of RNA. Its role in RNA transport was first demonstrated by overexpression of the FG-rich C-terminal domain of the protein, causing an accumulation of poly(A)$^+$ RNA in the nucleus (Bastos *et al*., 1996). It was later shown that when an anti-Nup153 antibody was injected into *Xenopus* oocytes, poly(A)$^+$ RNA, 5S ribosomal (r)RNA, U1 small nuclear RNA, and the HIV Rev complex, but not tRNA or importin β, accumulated in the nucleoplasm (Ullman *et al*., 1999). However, it remained unclear from these early studies whether such an export block might have occurred at the NPC core, the nuclear basket, or even deeper within the nuclear interior.

To further explore the role of Nup153 in RNA export, especially in the context of the nuclear basket, we have studied the nucleocytoplasmic translocation of a specific mRNP particle, the Balbiani ring (BR) granules in the salivary glands of the dipteran *Chironomus tentans*. The BR granules, 50 nm in diameter, can be identified in the electron microscope, and the translocation through the nuclear pore can be visualized (Daneholt, 1997, 2001). We have now studied how injection of antibodies against the N-terminal domain of Nup153 affects the translocation of BR RNP through the nuclear pores. The antibody blocked the transport of BR RNA, and BR mRNP particles were arrested on top of the basket fibrils, i.e., at the distal end of the basket fibrils. Evidently, the particles bound to the basket from the top but were not able to enter into the basket. Remarkably, this effect by Nup153 seems to be exerted from a distance, and possible mechanisms are being considered. The binding of the antibody did not prevent the RNP particles that had entered the basket to complete their translocation through the NPC. It was also observed that ribosomal subunits accumulated in nucleoplasm and did not enter nuclear baskets upon injection of anti-Nup153, indicating that ribosomal subunits behave as mRNPs at and within the nuclear basket.

MATERIALS AND METHODS

Experimental Material

C. tentans salivary glands were isolated from rapidly growing fourth instars raised under laboratory conditions. A *C. tentans* epithelial cell line was cultured at 24°C as described previously (Wyss, 1982).

Antibodies and DNA Probes

Mouse monoclonal antibody (mAb) PF190 × 7A8 was raised against rat Nup153 and shows high specificity to Nup153 in various organisms (Cordes *et al*., 1993). The rat Nup153 epitope was mapped within the N-terminal domain between amino acids 439 and 611 (Hase and Cordes, 2003). mAb 414 was from Covance (BAbCO, Berkeley, CA), and the monoclonal human factor VIII antibody was from DakoCytomation Denmark (Glostrup, Denmark). Rabbit polyclonal Tpr antibodies were raised against recombinant *Xenopus* Tpr C-terminal domain polypeptides. Rabbit affinity-purified polyclonal SCP3 antibodies were provided by Christer Höög (Karolinska Institutet, Stockholm, Sweden). Secondary antibodies coupled to horseradish peroxidase and fluorochromes were from DakoCytomation Denmark, and those coupled to 12 nm colloidal gold were from Jackson ImmunoResearch Laboratories (West Grove, PA).

Fluorescent DNA probes used for in situ hybridization were from Thermo BioSciences (Ulm, Germany). The BR mRNA probe was a Cy3-coupled 30 oligomer (ACTTGGCTTGCTGTGTTTGCTTGGTTTGCT), the 18S rRNA probe was a Cy3-coupled 21 oligomer (TTTCAGTCCACAATCCCAACT), and the 28S rRNA probe was a fluorescein isothiocyanate (FITC)-coupled 33 oligomer (CATTCGAATATTTGCTACTACCACCAAGATCTG).

Antibody Purification and Concentration

For microinjection and immunoelectron microscopic studies, hybridoma supernatant of the Nup153 antibody PF190 × 7A8 was concentrated and purified on a HiTrap Protein G affinity column (GE Healthcare, Little Chalfont,

Buckinghamshire, United Kingdom). Bound antibodies were eluted with 0.1 M glycine-HCl, pH 2.7, neutralized with 1 M Tris, pH 9.0, and further concentrated by ultrafiltration using a 50-kDa molecular weight Centriplus column (Millipore, Billerica, MA), with concomitant buffer exchange for phosphate-buffered saline (PBS). The final concentration of the purified antibody was 12 mg/ml.

Western Blot Analysis of Nuclear Extracts

Tissue culture cells were washed twice in cold PBS before disrupting the cells in TNM buffer (1 mM $MgCl_2$ and 100 mM NaCl in 10 mM tetraethylammonium-HCl, pH 7.0) with 0.2% Nonidet P-40 and Complete protease inhibitor cocktail (Roche Diagnostics, Basel, Switzerland). The extract was homogenized and then centrifuged at 2000 × *g* and 4°C for 10 min. The pellet containing the nuclei was resuspended in TNM buffer with protease inhibitors, sedimented by centrifugation again, and suspended in PBS and protease inhibitors. After brief sonication, the suspension was boiled in protein sample buffer. Proteins were separated by SDS-PAGE on 7.5% polyacrylamide gels and blotted onto Immobilon-P membranes (Millipore, Solna, Sweden) Blocking of filters and incubations with primary and secondary antibodies were performed essentially as described previously (Zhao *et al*., 2002).

Immunofluorescence Microscopy

Immunofluorescence microscopy was performed on salivary glands isolated from larvae by decapitation. The glands were placed on polyvinyl-treated (1 mg/ml) coverslips, fixed, and permeabilized in −20°C methanol for 5 min, washed in PBS, and blocked in 5% milk and 5% bovine serum albumin (BSA) in PBS at room temperature for 1 h. Subsequent incubations with primary antibodies were in PBS with 0.5% milk and 0.5% BSA for 1 h, followed by three washes in PBS of 5 min each, and incubations with secondary antibodies for 45 min. DNA staining was with SYTOX orange nucleic acid stain (Invitrogen, Carlsbad, CA) and 4,6-diamidino-2-phenylindole (DAPI). After two further washes in PBS of 5 min each, the specimens were mounted in Vectashield mounting media (Vector Laboratories, Burlingame, CA) and examined in a laser scanning confocal microscope (Zeiss LSM 510; Carl Zeiss, Oberkochen, Germany), using *z*-axis optical sections of ~1-μm thickness.

Immunoelectron Microscopy

Larval salivary glands were fixed at room temperature for 30 min in 4% formaldehyde and 0.1% glutaraldehyde in 0.1 M cacodylate buffer, pH 7.2. The glands were washed in cacodylate buffer and then dehydrated in ethanol solutions (70, 90, 95, and 100%). Subsequent embedding in the resin LR White (London Resin, Reading, United Kingdom), preparation of ultrathin sections, and immunogold labeling were performed as described previously (Krull *et al*., 2004).

Microinjection and Electron Microscopy

Isolated salivary glands were placed in a minimum amount of ZO medium (Wyss, 1982) surrounded by paraffin oil. The gland cell nuclei were injected by a micromanipulator (Eppendorf 5170; Eppendorf, Hamburg, Germany) and a transjector (Eppendorf 5246) with Eppendorf capillary femtotips (Femtotip II). The injection was done for 1.5 s at 800 hPa for the antibody solution and at 400 hPa for the PBS solution. The antibody was diluted to 9 mg/ml in PBS and occasionally mixed with 10 mg/ml dextran coupled to FITC (4 and 40 kDa; Sigma-Aldrich, Stockholm, Sweden). As controls, mock injections were performed with 10 mg/ml dextran-FITC molecules in PBS and with PBS only. The glands were further incubated in 30 μl of fresh hemolymph in a humid chamber at 18°C for 90 min. The gland was then fixed in 0.1 M Na-cacodylate buffer, pH 7.2, with 2% glutaraldehyde and 0.05 M sucrose at 4°C for 2 h; rinsed in 0.1 M Na-cacodylate buffer, pH 7.2, with 0.05 M sucrose at 4°C overnight; and postfixed in 0.1 M Na-cacodylate buffer with 1% osmium tetroxide for 1 h. The gland was further rinsed in the same buffer with sucrose and then dehydrated stepwise in ethanol (70, 90, 95, and 99%). The glands were transferred into a 1:3 mixture of an Agar 100 resin kit (Agar Scientific, Stansted, United Kingdom) and 99% ethanol for 30 min and then incubated in a 1:1 mixture of the Agar 100 kit and ethanol overnight, and finally in undiluted Agar 100 kit for 3–8 h. The gland was then cut into portions containing both injected and noninjected cells. The tissue pieces were then placed in gelatin capsules containing the Agar 100 resin kit and polymerized at 45°C for 48 h and at 60°C for 72 h.

In Situ Hybridization

Microinjected glands were fixed at room temperature in 0.1 M cacodylate buffer, pH 7.2, with 4% formaldehyde for 60 min and then trimmed so that only the segment with the microinjected cells was left. This segment was cryoprotected with 2.3 M sucrose in 0.1 M cacodylate buffer and frozen by immersion in liquid nitrogen. Semithin cryosections of 1 μm thickness were picked up on drops of 2.3 M sucrose in cacodylate buffer and deposited on slides treated with Alcian blue (Carl Roth, Karlsruhe, Germany). The specimens were then washed in PBS, refixed in 4% formaldehyde in PBS for 10 min, again washed in PBS, and then acetylated in freshly made acetylation buffer (1.3% triethanolamine and 0.25% acetic anhydride) for 10 min. After further washes in PBS, the specimens were prehybridized with hybridization buffer (25% formamide, 4× SSC, 5× Denharts buffer, 250 μg/ml yeast tRNA [Sigma-Aldrich], 500 μg/ml denatured salmon sperm DNA [Sigma-Aldrich], and 1 mM EDTA) in a humid chamber soaked with 4× SSC and 25% formamide at room temperature for 4 h. The actual hybridization in hybridization buffer with 1.2 μg/ml fluorescent DNA probes was performed overnight at 45°C, followed by brief washes in 5× SSC and in 0.2× SSC at 45°C for 1 h. Chromosomal DNA was labeled with DAPI. The specimens were washed for 3 × 5 min in 0.2× SSC at room temperature, mounted in Vectashield, and examined in a Leica DMRA2 microscope (Leica, Wetzlar, Germany). Digital image collection and processing was with a Hamamatsu C4742-95 charge-coupled device camera (Hamamatsu, Bridgewater, NJ) and the Openlab 3.0.7 software package from Improvision (Coventry, England).

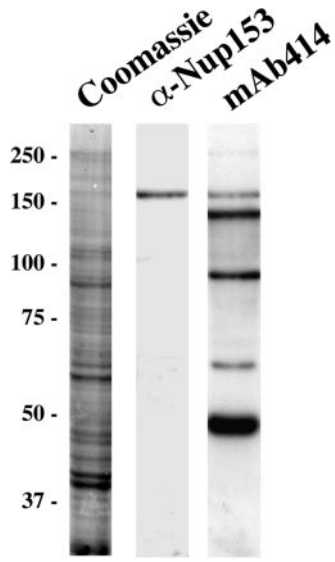

Figure 1. Immunoblot analysis of nuclear extract from *C. tentans* tissue culture cells using antibodies specific for Nup153 and other FG-repeat nucleoporins. Proteins separated by SDS-PAGE on neighboring lanes were probed with Nup153 mAb PF190 × 7A8 and mAb 414. Coomassie blue-stained nuclear extract proteins are shown as reference. Relative positions of molecular mass standards in kilodaltons are indicated to the left.

RESULTS

Identification of C. tentans *Nup153*

To study Nup153 in *C. tentans*, we used a mAb that recognizes the N-terminal domain of Nup153. The specificity of the antibody was first tested on a *C. tentans* total nuclear extract from tissue culture cells by Western blot analysis (Figure 1). The antibody interacted specifically with a single band at ~160 kDa, i.e., with a protein of similar size as Nup153 from different vertebrate species. The same extract was probed with mAb414, an antibody known to recognize Nup153 and other nucleoporins in various organisms (Sukegawa and Blobel, 1993). One of the bands recognized by the antibody migrated in parallel with the one recognized by the anti-Nup153 antibody, strengthening the assumption that the antibody specifically recognizes the *C. tentans* Nup153 homologue.

The antibody was further tested by immunofluorescence microscopy on salivary glands. A nuclear rim was clearly seen, whereas the nucleoplasm was only faintly stained (Figure 2), with no apparent staining of the chromosomes or in the cytoplasm. Thus, the cellular distribution agrees with the one predicted for a Nup153 protein. Together, these results indicate that the antibody raised against rat-Nup153 also recognizes a *C. tentans* homologue of Nup153.

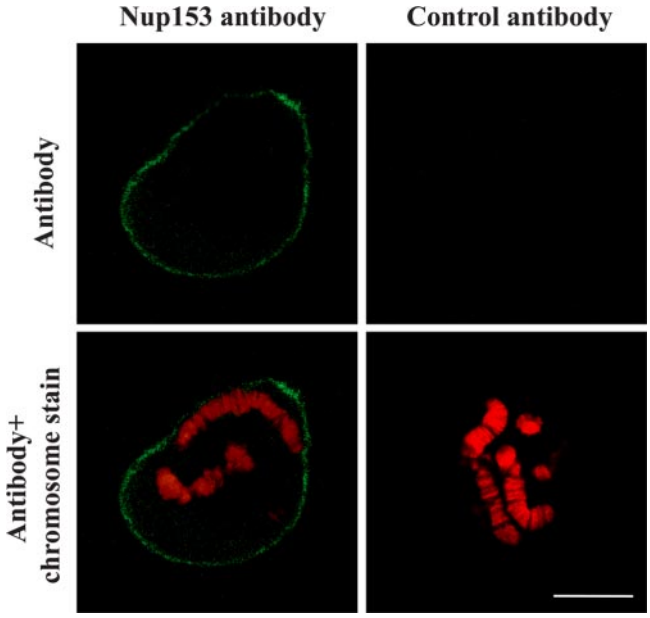

Figure 2. Immunofluorescence microscopy of salivary gland cells using anti-Nup153 and FITC-coupled secondary antibodies. A mAb against human factor VIII was used as negative control. The chromosomes are stained with SYTOX orange nucleic acid stain. Bar, 20 μm.

Nup153 Is Located on the Nuclear Side of the NPC Core

A closer look at the distribution of Nup153 was performed by immunoelectron microscopy on sections of larval salivary glands. We adopted a recently described postembedding approach (Krull *et al*., 2004). The monoclonal Nup153 antibody was used as primary antibody, a monoclonal human factor VIII antibody as control antibody, and a gold-conjugated anti-mouse IgG as secondary antibody.

The immunolabeling for Nup153 was essentially restricted to the nuclear envelope (NE), which is seen in the low-magnification image presented in Figure 3A, arrows. The immunosignal over the NE was found to be >50 times higher than the background signal in adjacent nucleoplasm and cytoplasm (gold particles per area unit measured), whereas the control antibody produced essentially no NE staining. Thus, the ultrastructural data further support the conclusion that also *C. tentans* Nup153 is predominantly located at the NE.

To more precisely establish the location of the gold particles, we examined the NE at higher magnification. The morphology of an NPC and its relation to the NE is displayed in Figure 3B. The two membranes of the nuclear envelope are seen as white lines (nonstained) that fuse at the nuclear pore. The pore itself is filled with tightly packed material constituting the core of the NPC. Fibrous material representing the nuclear basket is seen attached to the nuclear side of the NPC core. Two representative examples of NPCs, immunolabeled for Nup153, are shown in Figure 3, C and D, with gold grains seen bound to the NPC core. To semiquantitatively determine the location of the gold particles, we measured the position of 65 particles in relation to the horizontal mid-axis through the NPC. Only such gold-labeled pores were evaluated in which the cross-section was essentially perpendicular to the neighboring NE and where both NE membranes were discernible. The distances of the gold grains relative to the NPC and NE midplane are presented in Figure 4B, along with a schematic drawing of the NPC in Figure 4A. This allows direct comparison of gold grain positions relative to the NPC and basket structure shown in scale. Nup153 gold particles are found mainly distributed over the core of the NPC, with a clear preference for the nuclear side. As the primary antibody–secondary antibody complex can freely rotate on top of the plastic surface in this postembedding approach, the Nup153 epitope is likely to be located close to the center of the gold grain distribution, i.e., on the nuclear side of the NPC core. This result is in good agreement with previous studies (Sukegawa and Blobel, 1993; Walther *et al*., 2001; Fahrenkrog *et al*., 2002; Krull *et al*., 2004) in which vertebrate Nup153 has been shown to be located on the nuclear surface of the NPC core.

Because Nup153 is known to interact with the nuclear basket protein Tpr (Hase and Cordes, 2003), we wanted to compare the immunogold labeling patterns for both proteins. To label Tpr, we used a polyclonal antibody against the C-terminal domain of Tpr that was known to cross-react between species. In Western blot analysis of *C. tentans* nuclear extracts, the antibody recognized a Tpr-sized protein of >200 kDa (our unpublished data). The distribution of Tpr in salivary glands was subsequently investigated by immunoelectron microscopy. In this case, a polyclonal SCP3 antibody served as control antibody and a gold-labeled anti-rabbit antibody as secondary antibody. The majority of gold grains was found in the immediate vicinity of the NE, with >20 times higher signal intensity at the nuclear side of the NE than in adjacent nucleoplasm and cytoplasm (particles per unit area; a 150-nm broad zone on each side of the NE was included in the NE measurement). In the control specimens, the immunosignal was negligible. Two examples of the location of Tpr gold particles in relation to the NPC are displayed in Figure 3, E and F. In addition, the position of 63 particles was measured as described above, and the results are shown as a diagram in Figure 4C. In contrast to the rather narrow distribution and sharp peak of Nup153 immunogold grains, the distribution of the Tpr immunogold particles was broader. However, the distribution was clearly congruent to the area occupied by the nuclear basket, with a clear preference for the terminal ring region. We therefore conclude that Tpr in *C. tentans* salivary gland cells is present in the basket and that the C terminus of Tpr is preferentially located at the top of the basket, in agreement with results obtained in other species (Frosst *et al*., 2002; Krull *et al*., 2004).

Injection of an Nup153 Antibody Blocks Export of Both Messenger and rRNA

After having localized the Nup153 antibody target site at the NPC, we used this antibody for microinjection experiments to study the effects on RNA export. Nuclei in salivary glands were injected with the antibody, and the glands were then incubated in hemolymph for 90 min. Semithin cryosections of mildly fixed glands were prepared and used for in situ hybridization with fluorescently labeled anti-sense DNA probes. Adjacent cells, either noninjected or mock injected with PBS, served as internal controls.

In non- and mock-injected cells, the BR antisense mRNA probe, coupled to the red dye Cy3, specifically recognized and intensely stained the highly transcriptionally active BR (Figure 5, top left). Other regions of the nucleoplasm were only weakly stained, whereas some more labeling was seen in the cytoplasm. The association of the BR with a chromosome was shown by chromosomal labeling, using the DNA dye DAPI (Figure 5, bottom left). On the other hand, the antisense 28S rRNA probe, coupled to the green dye FITC,

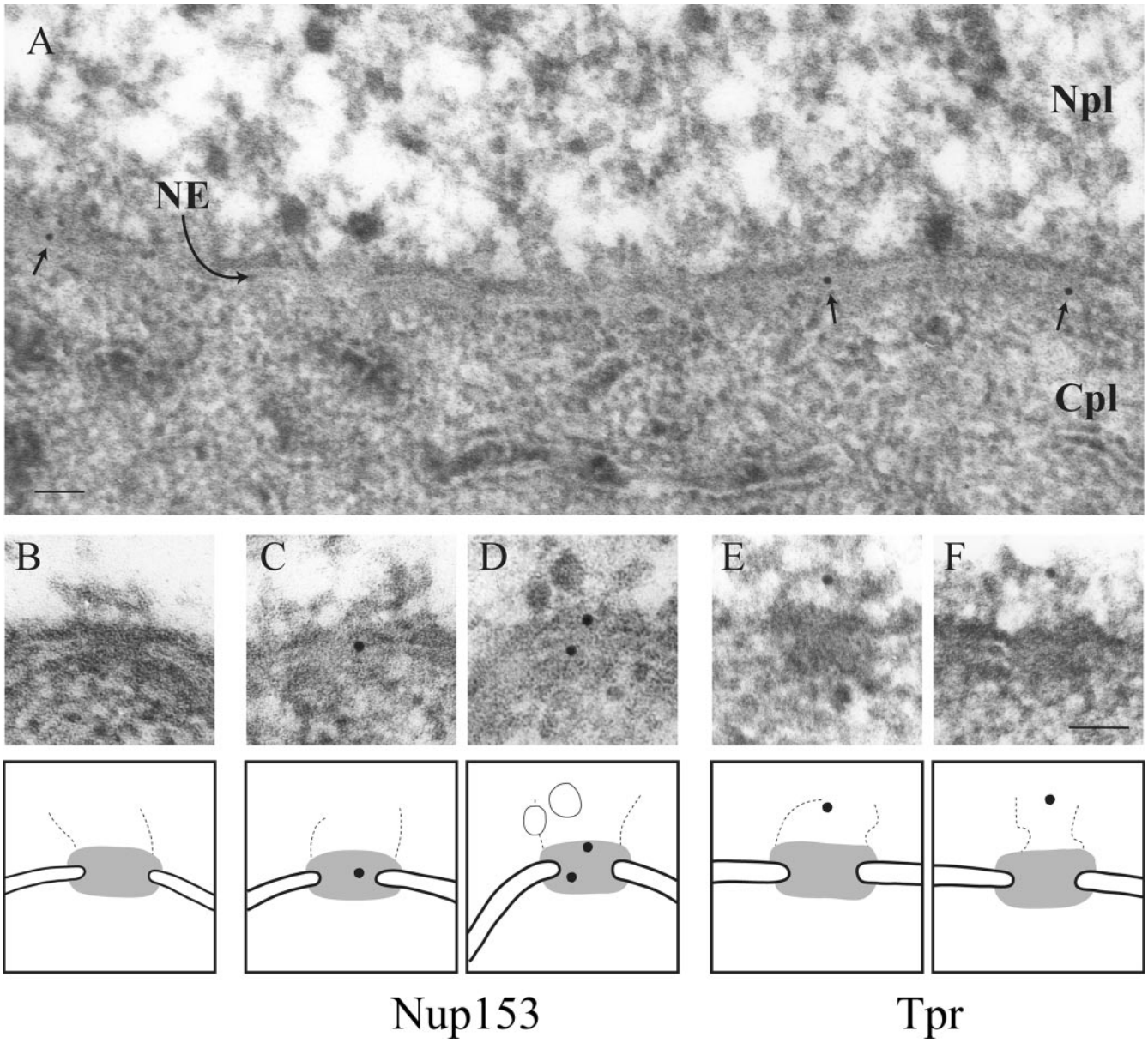

Figure 3. Localization of Nup153 and Tpr at the nuclear pore complex by postembedding immunoelectron microscopy. Primary antibodies (anti-Nup153 or anti-Tpr) were visualized with secondary antibodies coupled to colloidal gold. Immunolabeling with anti-Nup153 (A, C, and D) and with anti-Tpr (E and F). A segment of the NE as well as adjacent regions of nucleoplasm (Npl) and cytoplasm (Cpl) are displayed in A. Two large BR particles are bound to the nuclear side of the NE (left), and one particle has started to translocate through the nuclear pore (right). Gold particles at the NE are marked by arrows. In B–F, micrographs of single NPCs are presented. Corresponding schematic drawings are shown below. The core of the NPC is depicted in gray and the approximate position of the nuclear basket has been demarcated by broken lines. In B, a representative NPC is displayed in which the electron-dense NPC core, the flanking double membranes of the NE, and fibrous basket components attached to the nuclear side of the NPC can be discerned. Bars, 100 nm.

gave a moderately strong fluorescence signal above the nucleolus, only traces of labeling in other regions of the nucleoplasm, but intense staining of the entire cytoplasm (Figure 5, middle left).

After microinjection of the Nup153 antibody, the fluorescence patterns changed dramatically (Figure 5, right). The nucleoplasm became heavily stained with the BR mRNA probe (Figure 5, top right), and a striking increase in the labeling intensity of the nucleoplasm was notable with the 28S rRNA probe as well (Figure 5, middle right). These results pointed at a conspicuous inhibition of messenger and rRNA export by the Nup153 antibody. The labeling of BRs (our unpublished data) and nucleoli (Figure 5, middle right) did not change, indicating that transcription was not altered.

To assess whether the antibody effects might be due to unspecific clogging of the pore, we tested whether inert macromolecules can diffuse through the pore. FITC-coupled dextran molecules with a molecular mass of 4 or 40 kDa were injected into salivary gland nuclei either in PBS alone or together with the Nup153 antibody (see Supplemental Figure). These results demonstrated that the pores were still

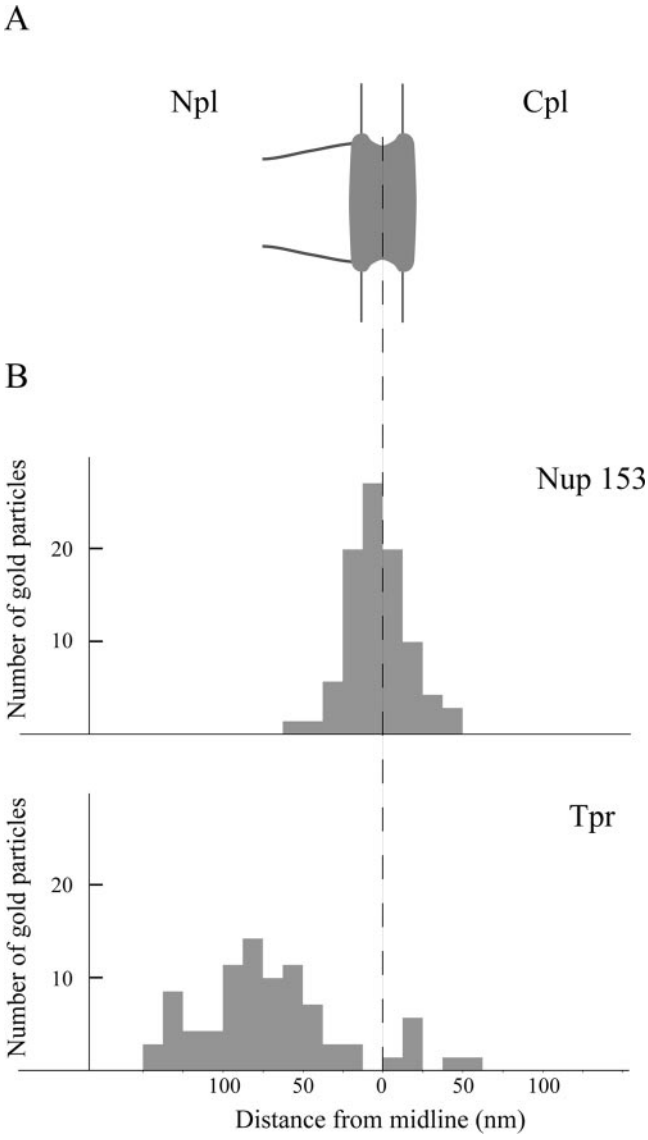

Figure 4. Immunogold labeling of Nup153 and Tpr in relation to the midplane of NE. (A) Schematic drawing of an NPC. The core and basket of the NPC have been outlined, and nucleoplasm (Npl) and cytoplasm (Cpl) have been indicated. The vertical broken line represents the midline of the NE. (B and C) Distribution of immunogold labeling for Nup153 (B) and Tpr (C) relative to the NE midline. The distance of the gold particles from the NE midline is displayed on the *x*-axis, and the number of particles on the *y*-axis. The histograms in B and C can be directly related to the drawing of the NPC in A.

able to allow passage of macromolecules of at least 4 kDa in the presence of the Nup153 antibody.

The Nup153 Antibody Causes an Export Block at an Early Stage of Translocation

To further study the nature of the export block, the distribution of the Balbiani ring RNP particles and ribosomal subunits in the nucleoplasm and at the NE was studied by electron microscopy (EM). After the injection of the Nup153 antibody into nuclei of salivary gland cells, and the incubation of these glands in hemolymph for 90 min, the glands were examined by EM. The injected cells were compared with adjacent PBS- and noninjected cells, which served as internal controls.

In the nucleoplasm of control cells, the BR RNP particles, 50 nm in diameter, can be readily encountered (arrows), whereas ribosome-sized RNP particles seem to be essentially absent (Figure 6, A and B). This result is in good agreement with the in situ hybridization data (Figure 5) and with previous biochemical analysis of rapidly labeled RNA in the nucleoplasm (Daneholt and Hosick, 1973). On injection of the Nup153 antibody, the BR RNP particles increase in number (bigger arrows), and simultaneously granular RNP particles, 20–30 nm in diameter, occur in large amounts (small arrows) (Figure 6F; higher magnification in Figure 6G). These results agree with the in situ hybridization data and support the conclusion that the Nup153 antibody causes a block in mRNA and rRNA export.

The translocation of a BR RNP particle through the nuclear pore could be followed in the control cells, which confirms previous observations (Daneholt, 1997). The BR particle passes through the nuclear basket as a spherical particle (Figure 6C) and docks in front of the channel (Figure 6E, particle to the left). When the particle starts to translocate, it elongates and enters the channel (Figure 6D). Later during translocation, the RNP particle looks like as a short ribbon and reaches into the cytoplasm (Figure 6E, particle to the right).

On injection of the anti-Nup153 antibody, the BR mRNP particles accumulate close to the nuclear side of the NE (Figure 6F). To get a semiquantitative measure of this increase, we compared antibody-injected and control cells with respect to the number of nuclear BR mRNP particles present within a distance of 150 nm from a central plane through the NE. In the presence of the Nup153 antibody, we found a more than twofold increase in the number of particles within this region (Table 1). Thus, the BR particles seemed to be selectively retained within this region. A close inspection of the BR particles and their relation to the NPCs revealed that the particles were located directly on top of the nuclear baskets (Figure 6, H–J). Apparently, the particles were capable of physically interacting with the distal end of the basket fibers but evidently could no longer move into the basket (cf. Figure 6, C–E).

Remarkably, no BR particles could be seen unfolding and translocating through the nuclear pores in the antibody-injected cells (Figure 6F), which is in sharp contrast to the situation in the control cells (Figure 6A and Table 2). We conclude that RNP particles that had already entered the basket or the NPC channel (Figure 6, C–E) were able to complete the translocation in the presence of the antibody (Figure 6, H–I).

Together, these results demonstrated that injection of a Nup153 antibody results in an export block at a stage between the binding of the BR particle to the basket and the further translocation of the particle into the basket, whereas particles engaged in translocation complete their passage through the pore.

DISCUSSION

In the present study, we have investigated the effect of antibodies to Nup153 on the nucleocytoplasmic translocation of BR mRNPs and ribosomal subunits through the nuclear pore. The main result is that the antibody blocks transport of a BR mRNP in a specific manner: the particle can bind to the top of the nuclear basket, but it cannot penetrate into the basket. Remarkably, Nup153 seems to exert its effect from a distance as the antibody target is

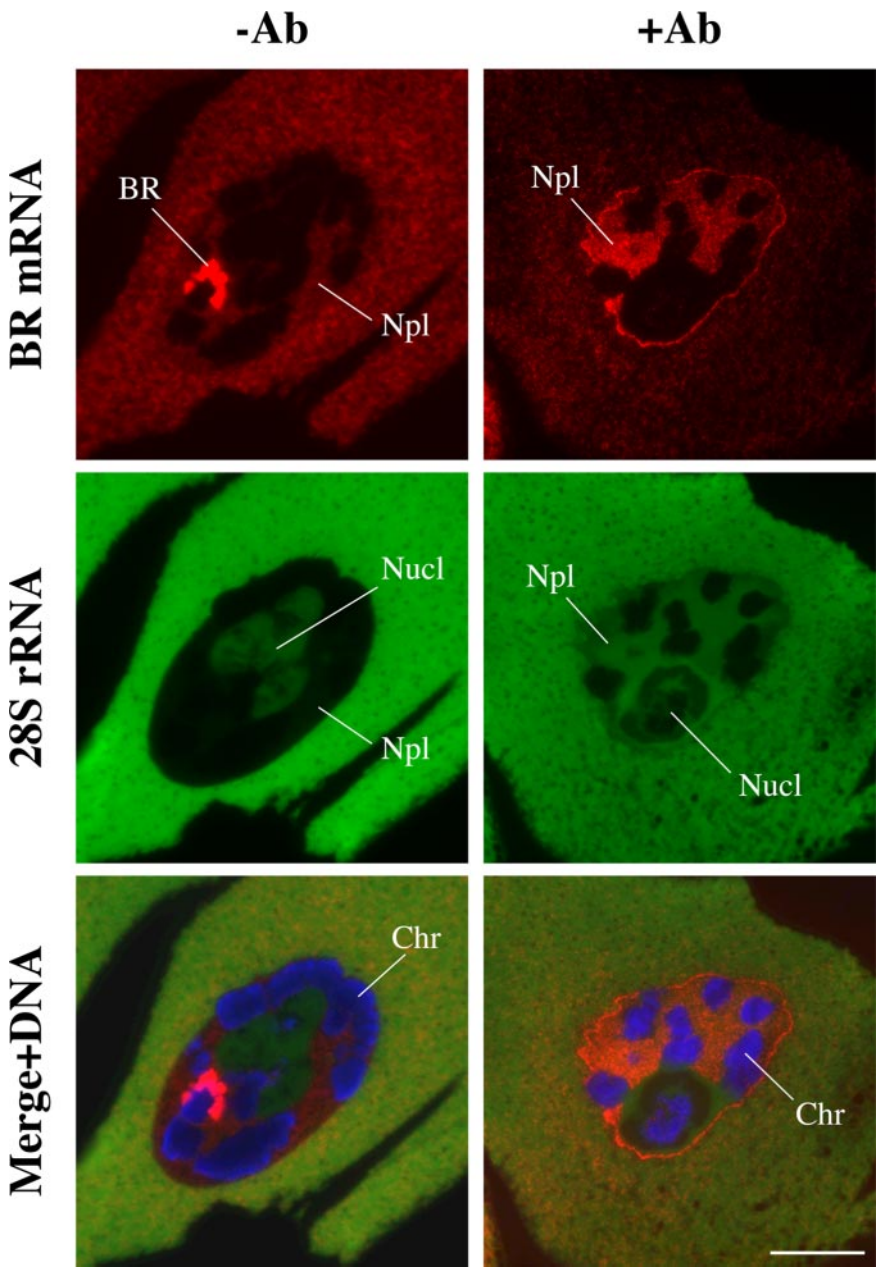

Figure 5. Effect of intranuclear injection of anti-Nup153 on the distribution of Balbiani ring transcripts and rRNA as studied by fluorescent in situ hybridization. BR mRNA is visualized with a Cy3-coupled complimentary oligonucleotide (red), and a FITC-coupled complimentary oligonucleotide (green) is used to label 28S rRNA in the same cells. The merged picture includes the DAPI staining for the polytene chromosomes (blue). Mock- and antibody-injected cells are shown to the left and right, respectively. BR, Balbiani ring; Chr, chromosome; Nucl, nucleolus; Npl, nucleoplasm. Bar, 20 μm.

located at the base of the basket. Our study also suggests that the antibody affects the transport of ribosomal subunits in a similar way.

Location of Nup153 and Tpr

The immuno-EM experiments showed that *C. tentans* Nup153 is part of the NPC core. Although the immunogold distribution covered the entire NPC core, the peak was on the nuclear side. The rather broad distribution around this central region can be explained by the indirect immunolabeling approach and by various geometric factors (for discussion, see Krull *et al.*, 2004). Together, our results are in good agreement with recent studies locating Nup153 to the nuclear ring of the NPC (Walther *et al.*, 2001; Fahrenkrog *et al.*, 2002; Krull *et al.*, 2004). Furthermore, because Nup153 can interact with the basket protein Tpr in vertebrates (Walther *et al.*, 2001; Hase and Cordes, 2003; Krull *et al.*, 2004), it seems likely that Nup153 anchors the basket to the nuclear ring also in *C. tentans*. However, at present we cannot exclude that some Nup153 molecules can be mobile within the NPC core and even reach the cytoplasmic side of the NPC as suggested by others (Nakielny and Dreyfuss, 1999; Fahrenkrog *et al.*, 2002).

It should also be emphasized that the Nup153 antibody used in this study is directed against the N-terminal domain of Nup153. It is therefore possible that the middle part and especially the C-terminal FG-repeat portions, that have little regular secondary structure and might therefore adopt a highly extended conformation, could project into the basket and even reach the top of the basket, as suggested recently (Fahrenkrog *et al.* 2002).

We confirmed by immunoelectron microscopy that Tpr is present in the basket, using an antibody to the C-terminal end of Tpr. The immunosignal is recorded above the nuclear

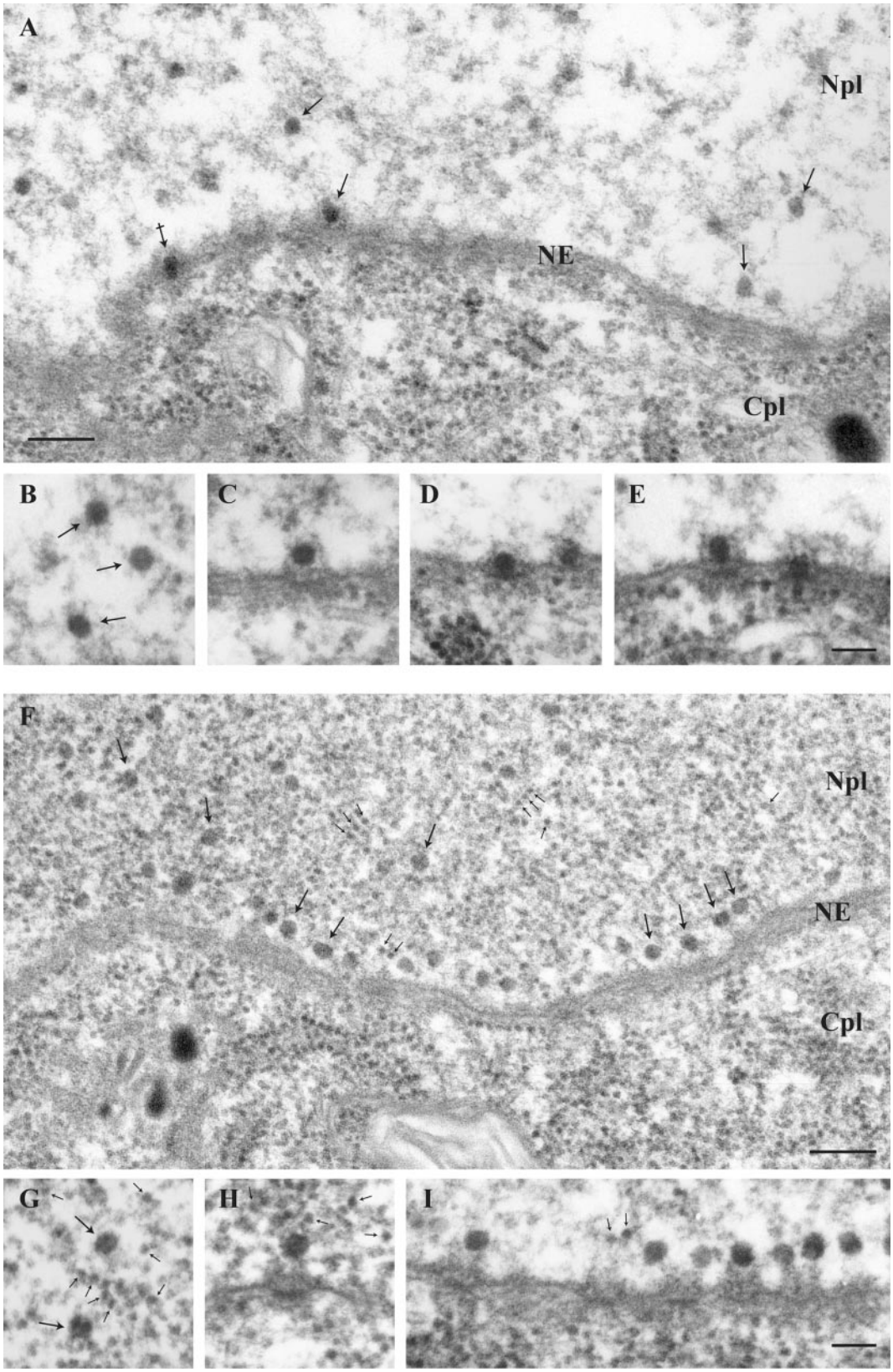

Figure 6. Effect of intranuclear injection of anti-Nup153 on the appearance of Balbiani ring granules in nucleoplasm and nuclear pores as studied by electron microscopy. Mock-injected cells are shown in A–E and antibody-injected cells in F–I. A and F represent overviews of a segment of the NE with adjacent nucleoplasm (Npl) and cytoplasm (Cpl), B and G show enlarged areas in nucleoplasm, and C–E and H–I show enlarged NE regions with NPCs. Some Balbiani ring granules have been marked by large arrows and a few ribosomes by small arrows. Bars, 200 nm (A and F) and 100 nm (E and I).

Table 1. Effect of injected anti-Nup153 on the number of BR particles bound to or present in the nuclear basket

Exp	Injection	No. of bound particles	Relative length of NE	No./length	α-Nup/control
1	α-Nup153	583	4.7	104	1.8
	Control	513	8.8	58	
2	α-Nup153	1057	9.3	114	2.0
	Control	440	7.7	57	

basket with a peak ~50 nm from the NPC core, corresponding to the position of the terminal ring region (Figure 4). The distribution of the C-terminal end of Tpr was, however, remarkably broad, which most likely reflects a considerable variability in the conformation of the basket (cf. e.g., the baskets in Figure 6, C and D). Clearly, the individual filaments are highly flexible, placing the terminal region at very different distances from the core of the NPC.

Binding of BR mRNPs to and Translocation through the NPC

Because the binding and translocation of the BR particles can be followed on the ultrastructural level, it has been feasible to describe this process in considerable detail (Daneholt, 1997). At higher resolution, the granular BR particle can be described as a short ribbon bent into a ring (Skoglund *et al.*, 1986) (Figure 7). The particle is asymmetric, which has been schematically indicated in Figure 7 by a thin 5′ and a thick 3′ end. When the passage through the pore is scrutinized, the process can be divided into several discrete steps: the BR particle binds to the nuclear basket, passes through the basket and docks in front of the central channel, the bent ribbon of the BR particle unrolls, and the extended ribbon translocates through the channel and exits into the cytoplasm. The 5′ end of the ribbon is always in the lead during the actual translocation process. Proteins are added to and displaced from the BR particle in conjunction with the passage through the nuclear pore (Daneholt, 2001).

The anti-Nup153 antibody blocks the export pathway of the BR mRNP at a step just subsequent to an initial binding step of the particle to the top of the basket. Because we did not find any BR particles in the basket itself or within the NPC, it seems as if all those present when the antibody was injected had been able to complete their passage through the NPC, suggesting that the antibody did not affect the interaction of the BR particle with the NPC core and the translocation through the NPC channel.

Because the antibodies bind to the base of the basket, whereas the BR particles are retarded on its top, i.e., at a distance >50 nm away, the question arises how this remote effect can be generated. It could be argued that the antibodies, bound to Nup153 at the base of the basket, block the entrance to the actual NPC channel and cause a unspecific pile-up of export cargo within the basket. However, if the

Table 2. Effect of injected anti-Nup153 on the number of BR particles translocating through the central channel of the nuclear pore complex

Exp	Injection	No. of translocating particles	Relative length of NE	No./length
1	α-Nup153	0	4.7	0
	Control	75	8.8	8.5
2	α-Nup153	0	9.3	0
	Control	47	7.7	6.1

Figure 7. Model of a BR mRNP particle's entry into and passage through the nuclear basket. Three phases in the passage of an BR RNP particle through the nuclear basket are displayed. Initially, the BR particle binds to Tpr C termini in the top of the basket, and a terminal ring is formed. The particle is then released and transferred into the basket; the terminal ring is dissolved. Finally, the BR particle is docked with its 5′ end in front of the entrance to the central channel. The BR particle is ringlike; to clearly point out the 5′ and 3′ ends of the particle, we have schematically presented the ends as a thin 5′ and a thick 3′ end. The basket architecture has been depicted according to Krull *et al.* (2004); note the position of the bifurcated C-terminal ends at the top. The Tpr fibrils are shown as single back-folded Tpr dimers. Nup 153 (in red) anchors the basket to the NPC core.

block were unspecific and at the base of the basket, large mRNPs and ribosomal RNPs would at least occasionally occur *within* the basket, but they do not. In addition, if other potential export cargo, e.g., proteins, had been accumulated within the basket after injection of the antibody, the clogged material would have been recorded as an increase in electron-dense material, which is not the case. Finally, inert macromolecules such as 4-kDa dextran can still readily pass through the NPCs when the transport of large RNPs is inhibited by the antibody. The conclusion that the observed block is not due to unspecific clogging of the pore is also in agreement with another study showing that nuclear injection of Nup153 antibodies inhibits RNA transport in a *specific* manner (Ullman *et al*., 1999). In this study, the transport of a Rev protein complex was blocked, whereas a complex of similar size, namely, tRNA together with its export receptor, was not. In view of these consistent observations, we conclude that the BR particle transport block elicited by injection of the Nup153 antibody is not due to unspecific steric hindrance but is rather due to specific interference with the function of Nup153.

It is possible that the export block caused by the Nup153 antibody is linked to the dynamic changes occurring at the top of the basket ensuing the arrival of a BR particle (Kiseleva *et al*., 1996). The distal end of the basket seems to adopt a ringlike conformation upon contact with this mRNP particle. Later, when the particle has passed on, this ringlike arrangement seems to dissolve again. Put in the terms of a recent model of the nuclear basket (Krull *et al*., 2004), this implies that the C-terminal domains of the Tpr homodimers attach to the RNP particle, whereas neighboring basket fibrils interdigitate in a dynamic manner via the bifurcated distal segments of their Tpr rod domains, thus forming the ringlike structure at the top of the basket. This arrangement of loosely interconnected Tpr polypeptides can adopt alternating conformations in the course of the BR particle translocation process (Figure 7).

Antibody binding to Nup153 at the base of the nuclear basket could affect the overall flexibility of the basket and its ability to undergo conformational changes possibly required for further translocation of the BR particle. Alternatively, it is also possible to envision a more direct role for Nup153, deduced from a model in which the N-terminal part of Nup153 is located at the base of the basket, whereas the C-terminal FG-containing part is thought to be extended, flexible and able to transiently interact with the distal end of the basket, i.e., with its ringlike terminal part (Fahrenkrog *et al*., 2002). The C terminus of Nup153 could then be directly involved in the reorganization of the top of the basket subsequent to the binding of the BR particle. Alternatively, as proposed by Fahrenkrog *et al*. (2002), the Nup153 FG-repeat domains could bind cargo molecules at the top of the basket, then pull them into the basket, and guide them to and even through the central NPC channel. If this latter scenario is true, it is plausible that injected Nup153 antibodies could interfere with such a cargo-handling process. It is, however, remarkable then that the antibody only affects an early step of the mRNP transfer process into the basket, resulting in an arrest on top of the basket, whereas subsequent steps in the translocation process seem to proceed normally in the presence of the antibody. We conclude that it remains to be established whether Nup153 affects the conformational dynamics of the basket as a whole or whether it is involved more directly via an extended C-terminal domain reaching the top of the basket.

It should also be noted that Nup153 has been reported being a highly mobile protein that can shuttle between different NPCs and the nucleoplasm (Daigle *et al*., 2001; Griffis *et al*., 2004). Thus, the translocation process could require an ongoing exchange of the NPC-bound Nup153 at the base of the basket for a mobile form of Nup153 in the nucleoplasm. However, our immunoelectron microscopic data did not provide evidence for such a pool of unanchored, nucleoplasmic Nup153 molecules in the vicinity of the nuclear basket. It was also evident that Nup153 proteins are not linked to the nucleoplasmic BR particles themselves, arguing against a role for Nup153 as a mobile export receptor for this type of cargo.

Transport of Ribosomal Subunits from Nucleoli to and through Nuclear Pores

Another striking observation in this study was that the export of the ribosomal subunits was blocked upon injection of the Nup153 antibody. This was evident from the heavy accumulation of 28S and 18S RNA in the nucleoplasm, as revealed by in situ hybridization, and the large amount of ribosome-sized granules in the nucleoplasm as seen in the electron microscope. It is known that the export receptor Crm1 is involved in transport of both the small and large subunits, which suggests that the ribosomal subunits pass through the central channel of the NPC core using the same FG-dependent translocation mechanism as mRNP particles (for reviews, see Fatica and Tollervey, 2002; Johnson *et al*., 2002; Cullen, 2003). Although there are differences between the pathways (Gleizes *et al*., 2001), it is possible that they partially converge. The present study supports such a concept, because both BR mRNP and ribosomal subunits accumulate in the nucleoplasm upon injection of the Nup153 antibody. However, because the concentration of the ribosomal subunits accumulated in the nucleoplasm was very high, it is difficult to decide whether there is, in fact, also an mRNP-like enrichment of ribosomal subunits on the top of the basket after antibody injection. It is, however, evident that the concentration of ribosomal subunits throughout nucleoplasm is much higher than *within* the basket (Figure 6F), suggesting that the same process operates at the top of the basket for both ribosomal subunits and mRNPs, making the RNPs translocation competent.

ACKNOWLEDGMENTS

The polyclonal SCP3 antibody was kindly provided by Christer Höög. We are grateful to Karin Askfors for technical assistance. The study was supported by the Swedish Research Council, Agouron Institute, European Community (3D-EM Network of Excellence), Human Frontier Science Program Organization, and Knut and Alice Wallenberg Foundation.

REFERENCES

Allen, T. D., Cronshaw, J. M., Bagley, S., Kiseleva, E., and Goldberg, M. W. (2000). The nuclear pore complex: mediator of translocation between nucleus and cytoplasm. J. Cell Sci. *113*, 1651–1659.

Bangs, P. L., Burke, B., Powers, C., Graig, R., Purohit, A., and Doxsey, S. (1998). Functional analysis of Tpr: identification of nuclear pore complex association and nuclear localization domains and a role in mRNA export. J. Cell Biol. *143*, 1801–1812.

Bastos, R., Lin, A., Enarson, M., and Burke, B. (1996). Targeting and function in mRNA export of nuclear pore complex protein Nup153. J. Cell Biol. *134*, 1141–1156.

Ben-Efraim, I., and Gerace, L. (2001). Gradient of increasing affinity of importin beta for nucleoporins along the pathway of nuclear import. J. Cell Biol. *152*, 411–417.

Cordes, V. C., Reidenbach, S., Köhler, A., Stuurman, N., van Driel, R., and Franke, W. W. (1993). Intranuclear filaments containing a nuclear pore complex protein. J. Cell Biol. *123*, 1333–1344.

Cordes, V. C., Reidenbach, S., Rackwitz, H.-R., and Franke, W. W. (1997). Identification of protein p270/Tpr as a constitutive component of the nuclear pore complex-attached intranuclear filaments. J. Cell Biol. *136*, 515–529.

Cronshaw, J. M., Krutchinsky, A. N., Zhang, W., Chait, B. T., and Matunis, M. J. (2002). Proteomic analysis of the mammalian nuclear pore complex. J. Cell Biol. *158*, 915–927.

Cullen, B. R. (2003). Nuclear RNA export. J. Cell Sci. *116*, 587–597.

Daigle, N., Beaudouin, J., Hartnell, L., Imreh, G., Hallberg, E., Lippincott-Schwartz, J., and Ellenberg, J. (2001). Nuclear pore complexes form immobile networks and have a very low turnover in live mammalian cells. J. Cell Biol. *154*, 71–84.

Daneholt, B. (1997). A look at RNP moving through the nuclear pore. Cell *88*, 585–588.

Daneholt, B. (2001). Assembly and transport of a premessenger RNP particle. Proc. Natl. Acad. Sci. USA *98*, 7012–7017.

Daneholt, B., and Hosick, H. (1973). Evidence for transport of 75S RNA from a discrete chromosomal region via nuclear sap to cytoplasm in *Chironomus tentans*. Proc. Natl. Acad. Sci. USA *70*, 442–446.

Dreyfuss, G., Kim, V. N., and Kataoka, N. (2002). Messenger-RNA-binding proteins and the messages they carry. Nat. Rev. Mol. Cell. Biol. *3*, 195–205.

Dworetzky, S., and Feldherr, C. (1988)., Translocation of RNA-coated gold particles through the nuclear pores of oocytes. J. Cell Biol. *106*, 575–584.

Enarson, P., Enarson, M., Bastos, R., and Burke, B. (1998). Amino-terminal sequences that direct Nucleoporin Nup153 to the inner surface of the nuclear envelope. Chromosoma *107*, 228–236.

Fahrenkrog, B., and Aebi, U. (2003). The nuclear pore complex: nucleocytoplasmic transport and beyond. Nature Rev. Mol. Cell. Biol. *4*, 757–766.

Fahrenkrog, B., Maco, B., Fager, A. M., Koser, J., Sauder, U., Ullman, K. S., and Aebi, U. (2002). Domain-specific antibodies reveal multiple-site topology of Nup153 within the nuclear pore complex. J. Struct. Biol. *140*, 254–267.

Fatica, A., and Tollervey, D. (2002). Making ribosomes. Curr. Opin. Cell Biol. *14*, 313–318.

Franke, W. W., and Scheer, U. (1974). Structures and functions of the nuclear envelope. In: The Cell Nucleus, Vol. 1 (ed H Busch), New York: Academic Press, 219–347.

Frosst, P., Guan, T., Subauste, C., Hahn, K., and Gerace, L. (2002). Tpr is localized within the nuclear basket of the pore complex and has a role in nuclear protein export. J. Cell Biol. *156*, 617–630.

Galy, V., Gadai, O., Fromont-Racine, M., Romano, A., Jacquier, A., and Nehrbass, U. (2004). Nuclear retention of unspliced mRNAs in yeast is mediated by perinuclear Mlp1. Cell *116*, 63–73.

Gilbert, W., and Guthrie, C. (2004). The Glc7p nuclear phosphatase promotes mRNA export by facilitating association of Mex67p with mRNA. Mol. Cell *13*, 201–212.

Görlich, D., and Kutay, U. (1999). Transport between the cell nucleus and the cytoplasm. Annu. Rev. Cell Dev. Biol. *15*, 607–660.

Gleizes, P. E., Noaillac-Depeyre, J., Leger-Silvestre, I., Teulieres, F. Dauxois, J. Y., Pommet, D., Azum-Gelade, M. C., and Gas, N. (2001). Ultrastructural localization of rRNA shows defective nuclear export of preribosomes in mutants of the Nup82p complex. J. Cell Biol. *155*, 923–936.

Griffis, E. R., Craige, B., Dimaano, C., Ullman, K. S., and Powers, M. A. (2004). Distinct functional domains within nucleoporins Nup153 and Nup98 mediate transcription-dependent mobility. Mol. Biol. Cell *15*, 1991–2002.

Hase, M. E., Kuznetsov, N., and Cordes, V. C. (2001). Amino acid substitutions of coiled-coil protein Tpr abrogate anchorage to the nuclear pore complex but not parallel, in-register homodimerization. Mol. Biol. Cell *12*, 2433–2452.

Hase, M. E., and Cordes, V. C. (2003). Direct interaction with Nup153 mediates binding of Tpr to the periphery of the nuclear pore complex. Mol. Biol. Cell *14*, 1923–1940.

Huang, Y., Gattoni, R., Stevenin, J., and Steitz, J. A. (2003). SR splicing factors serve as adapter proteins for TAP-dependent mRNA export. Mol. Cell *11*, 837–843.

Johnson, A. W., Lund, E., and Dahlberg, J. (2002). Nuclear export of ribosomal subunits. Trends Biochem. Sci. *27*, 580–585.

Kiseleva, E., Goldberg, M. W., Daneholt, B., and Allen, T. D. (1996). RNP export is mediated by structural reorganization of the nuclear pore basket. J. Mol. Biol. *260*, 304–311.

Kiseleva, E., Goldberg, M. W., Allen, T. D., and Akey, C. W. (1998). Active nuclear pore complexes in *Chironomus*: visualization of transporter configurations related to mRNP export. J. Cell Sci. *111*, 223–236.

Krull, S., Thyberg, J., Björkroth, B., Rackwitz, H.-R., and Cordes, V. C. (2004). Nucleoporins as components of the nuclear pore complex core structure and Tpr as the architectural element of the nuclear basket. Mol. Biol. Cell *15*, 4261–4277.

Lei, E. P., and Silver, P. A. (2002). Protein and RNA export from the nucleus. Dev. Cell *2*, 261–272.

Mehlin, H., Daneholt, B., and Skoglund, U. (1992). Translocation of a specific premessenger ribonucleoprotein particle through the nuclear pore studied with electron microscope tomography. Cell *69*, 605–613.

Nakielny, S., and Dreyfuss, G. (1999). Transport of proteins and RNAs in and out of the nucleus. Cell *99*, 677–690.

Nakielny, S., Shaikh, S., Burke, B., and Dreyfuss, G. (1999). Nup153 is an M9-containing mobile nucleoporin with a novel Ran-binding domain. EMBO J. *18*, 1982–1995.

Reed, R., and Hurt, E. (2002). A conserved mRNA export machinery coupled to pre-mRNA splicing. Cell *108*, 523–531.

Ribbeck, K., and Görlich, D. (2002). The permeability barrier of nuclear pore complexes appears to operate via hydrophobic exclusion. EMBO J. *21*, 2664–2671.

Rout, M. P., Aitchison, J. D., Suprapto, A., Hjertaas, K., Zhao, Y., and Chait, B. T. (2000). The yeast nuclear pore complex: composition, architecture, and transport mechanism. J. Cell Biol. *148*, 635–651.

Rout, M. P., Aitchison, J. D., Magnasco, M. O., and Chait, B. T. (2003). Virtual gating and nuclear transport: the hole picture. Trends Cell Biol. *13*, 622–628.

Shah, S., Tugendreich, S., and Forbes, D. J. (1998). Major binding sites for the nuclear import receptor are the internal nucleoporin Nup153 and the adjacent nuclear filament protein Tpr. J. Cell Biol. *141*, 31–49.

Skoglund, U., Andersson, K., Björkroth, B. Lamb, M. M., and Daneholt, B. (1986). Three-dimensional structure of a specific pre-messenger RNP particle established by electron microscope tomography. Nature *319*, 560–564.

Snay-Hodge, C. A., Colot, H. V., Goldstein, A. L., and Cole, C. N. (1998). Dbp5/Rat 8p is a yeast pore-associated DEAD-box protein essential for RNA export. EMBO J. *17*, 2663–2676.

Stevens, B. J., and Swift, H. (1966). RNA transport from nucleus to cytoplasm in Chironomus salivary glands. J. Cell Biol. *31*, 55–77.

Strässer, K., and Hurt, E. (2000). Yra1p, a conserved nuclear RNA-binding protein, interacts directly with Mex67p and is required for mRNA export. EMBO J. *19*, 410–420.

Strawn, L. A., Shen, T., Shulga, N., Goldfarb, D. S., and Wente, S. R. (2004). Minimal nuclear pore complexes define FG repeat domains essential for transport. Nat. Cell Biol. *6*, 197–206.

Stutz, F., Bachi, A., Doerks, T., Braun, I. C., Seraphin, B., Wilm, M., Bork, P., and Izaurralde, E. (2000). REF, an evolutionary conserved family of hnRNP-like proteins, interacts with TAP/Mex67p and participates in mRNA nuclear export. RNA *6*, 638–650.

Stutz, F., and Izaurralde, E. (2003). The interplay of nuclear mRNP assembly, mRNA surveillance and export. Trends Cell Biol. *13*, 319–327.

Sukegawa, J., and Blobel, G. (1993). A nuclear pore complex protein that contains zinc finger motifs, binds DNA, and faces the nucleoplasm. Cell *72*, 29–38.

Suntharalingam, M., and Wente, S. R. (2003). Peering through the pore: nuclear pore complex structure, assembly, and function. Dev. Cell *4*, 775–789.

Ullman, K. S., Shah, S. Powers, M. A., and Forbes, D. J. (1999). The nucleoporin Nup153 plays a critical role in multiple types of nuclear export. Mol. Biol. Cell. *10*, 649–664.

Vasu, S. K., and Forbes, D. J. (2001). Nuclear pores and nuclear assembly. Curr. Opin. Cell Biol. *13*, 363–375.

Walther, T. C., Fornerod, M., Pickersgill, H., Goldberg, M., Allen, T. D., and Mattaj, I. W. (2001). The nucleoporin Nup153 is required for nuclear pore basket formation, nuclear pore complex anchoring and import of a subset of nuclear proteins. EMBO J. *20*, 5703–5714.

Wyss, C. (1982). *Chironomus tentans* epithelial cell lines sensitive to ecdysteroids, juvenile hormone, insulin and heat shock. Exp. Cell Res. *139*, 309–319.

Zeitler, B., and Weis, K. (2004). The FG-repeat asymmetry of the nuclear pore complex is dispensable for bulk nucleocytoplasmic transport in vivo. J. Cell Biol. *167*, 583–590.

Zhao, J., Jin, S.-B., Björkroth, B., Wieslander, L., and Daneholt, B. (2002). The mRNA export factor Dbp5 is associated with Balbiani ring mRNP from gene to cytoplasm. EMBO J *21*, 1177–1187.